Journal of Structural Geology, Vol. 14, No. 10, pp. 1193 to 1202, 1992
Printed in Great Britain

0191-8141/92 $05.00+0.00

The rotation of garnet porphyroblasts around a single fold, Lukmanier Pass, Central Alps

PETER VISSER and NEIL S. MANCKTELOW

Geologisches Institut, ETH-Zentrum, CH-8092, Zürich, Switzerland

(*Received* 8 *October* 1991; *accepted in revised form* 28 *April* 1992)

Abstract—The orientation of the straight internal foliation S_i within large (~ 5 mm) garnet porphyroblasts has been measured relative to the orientation of the external foliation S_e around a single antiform of ~0.5 m wavelength, which folds the dominant regional foliation. The internal foliation is not constant in orientation, but varies consistently both with position around the fold and with the porphyroblast ellipticity. The dip of S_i (hinge dip taken as zero) is consistently less than the dip of S_e; it increases with increasing dip of S_e and with increasing ellipticity of the porphyroblasts. S_i effectively defines a fold with an opening angle greater than that in the external foliation. The opening angle of this fold in S_i decreases with increasing porphyroblast ellipticity. The observed variation in the orientation of S_i can be explained qualitatively by a flattened flexural flow model for fold development, as could be expected for folding of a pre-existing, strongly anisotropic foliation. The measurements clearly demonstrate that rotation of porphyroblasts relative to geographical co-ordinates did occur during the development of this fold and that a model based on the classical theories of rotation of stiff inclusions in a weaker viscous matrix is most appropriate.

INTRODUCTION

THE geometry of porphyroblasts in deformed metamorphic rocks has been studied in considerable detail since early in this century (e.g. Schmidt 1918), both to establish the timing of crystal growth relative to deformation (e.g. Zwart 1960, Spry 1969, Olesen 1978) and to obtain information on the kinematics of progressive deformation (e.g. Mügge 1930, Ramsay 1962, Spry 1963, Zwart & Oele 1966, Rosenfeld 1968, 1970, Schoneveld 1977, 1979, Vernon 1987). Asymmetric relationships between the helicitic internal fabric of porphyroblasts (≡ internal foliation S_i) and the external fabric in the surrounding matrix (≡ external foliation S_e), asymmetric tails of recrystallized material, and asymmetric 'pressure shadows' have been used as indicators of the sense of rotation and hence of the sense of shear of the overall deformation (e.g. Simpson & Schmid 1983, Passchier & Simpson 1986). In general such geometries only establish a *relative* rotation: they do not directly determine whether the porphyroblast itself (together with its included internal foliation) rotated relative to geographical co-ordinates, if the external foliation rotated, or indeed if both rotated and the observed relative rotation resulted from differing rates of rotation between the internal and external foliation (e.g. Ramsay 1962, Rosenfeld 1970, Fyson 1975, Schoneveld 1979, Bell 1985, Vernon 1988, Bell & Johnson 1989, 1990, 1992, Johnson 1990).

Theories of rigid particle rotation developed from fluid mechanics (e.g. Jeffery 1922, Gay 1968, Ghosh & Ramberg 1976, Ferguson 1979) predict that the behaviour of individual isolated particles should depend on the vorticity of flow in the matrix (which can be conveniently represented by the kinematic vorticity number, e.g. Truesdell 1954, Passchier 1987), on the ellipticity (aspect ratio) of the particle and on its orientation. In particular, for two-dimensional flows (plane strain), a circular particle should rotate at a constant rate with an angular velocity equal to one-half of the flow vorticity, whereas a very elongate particle should approach the quite different behaviour of a passive marker line. The behaviour of a particle of intermediate ellipticity obviously lies between these two extremes (e.g. Ghosh & Ramberg 1976, Fernandez 1988). Because the most commonly studied porphyroblasts, namely garnets, generally have a low aspect ratio, whereas the external foliation is usually defined by platy phyllosilicates, the difference in rotational behaviour between such differently shaped particles during deformation generally results in a relative rotation between the porphyroblast and the external foliation.

The internal foliation within porphyroblasts has been shown by several studies (e.g. Ramsay 1962, Fyson 1975, 1980, Steinhardt 1989) to be quite constant in its geographical orientation, even in strongly folded regions. This led Ramsay (1962) to suggest that such folds, which commonly approach a similar fold style, may have developed by passive amplification during coaxial pure shear. In this model, equant porphyroblasts do not themselves rotate and the apparent rotation is due to the passive rotation of the fold limbs during fold amplification. Bell (1985) has taken this approach one step further, suggesting that rigid porphyroblasts do not rotate at all during deformation, even when there is an important rotational component to the bulk deformation. This model has rather radical implications: it would mean that the sense of shear determined in zones of rotational deformation from porphyroblasts (e.g. 'snowball' garnets), δ-clast geometries (e.g. Passchier & Simpson 1986) and even intrafolial asymmetric folds (e.g. Van Den Driessche & Brun 1987) would all be incorrect (cf. Bell & Johnson 1992).

This paper presents data on the orientation of the

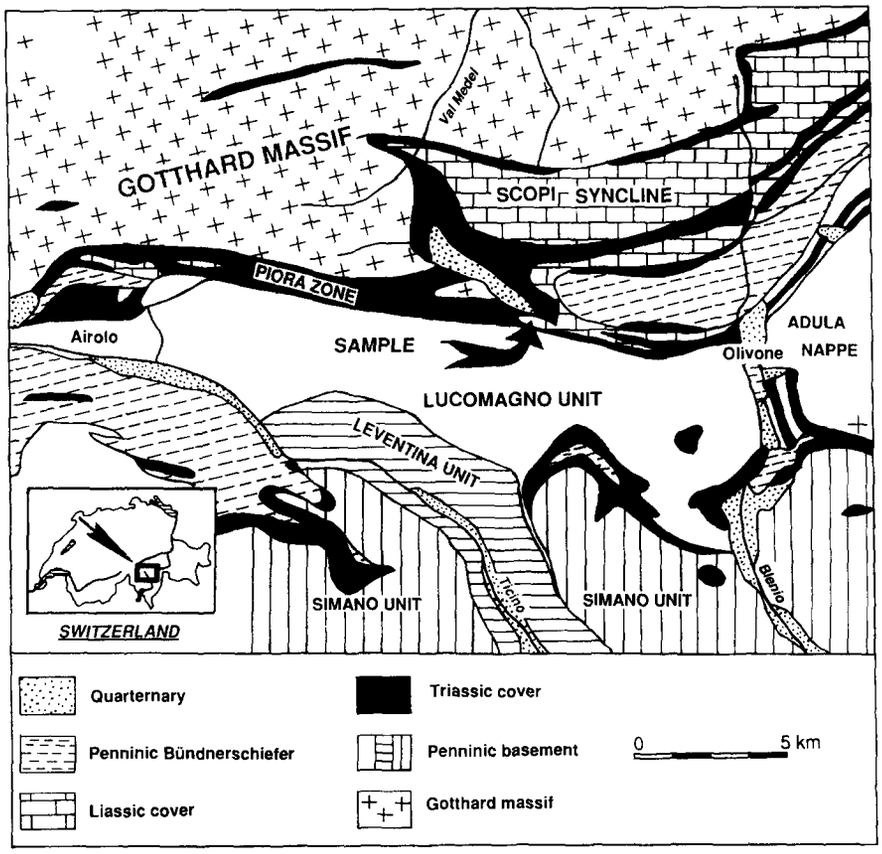

Fig. 1. Location diagram and simplified geological map of the Lukmanier Pass region. The location of the studied fold is indicated and corresponds to Swiss national grid co-ordinates 707.2/156.4.

internal foliation S_i in garnet porphyroblasts measured around a single fold from the Lukmanier Pass area of the Central Alps in Switzerland (Fig. 1). The orientation of S_i within these porphyroblasts has been analysed relative to position within the fold. These data provide a basis for discussing possible models of fold development in schistose, strongly anisotropic rocks.

GEOLOGICAL SETTING

The studied fold occurs within amphibolite facies garnet schists of the Stgir Series, which were originally shales of Liassic age forming part of the Mesozoic cover to the southern Gotthard Massif and adjacent Penninic basement (e.g. Chadwick 1965, Thakur 1973). The region has been subjected to four phases of Alpine deformation. The first deformation, D_1, produced isoclinal folding and imbricate stacking of basement and sedimentary cover units. This was followed by a pervasive phase of recumbent folding, D_2, in which overturned fold limbs commonly developed into major thrusts. The main penetrative foliation throughout the area developed at this time, associated with upper greenschist facies metamorphism south of the Gotthard Massif. The peak of thermal metamorphism post-dated D_2, with the growth of many porphyroblasts, including the garnets measured in this study (Figs. 2 and 3), indicating peak conditions of ~500–550°C at 5 kbar (Fox 1974, 1975, Adams *et al.* 1975, Frey 1978, Frey *et al.* 1980). The dominant regional S_2 schistosity is overprinted by a third folding phase D_3, with an associated weak to moderately developed crenulation cleavage. The studied fold belongs to this D_3 phase. Axial planes of D_3 folds in the Lukmanier area dip moderately to the northeast and fold axes plunge shallowly to the east-northeast. Minor garnet growth continued during the D_3 deformation, such that narrow rim regions to the porphyroblasts sometimes show a bending of the otherwise straight internal foliation into continuity with the external foliation (Fig. 2). A still younger, weak crenulation phase, D_4, can also be recognized in the Lukmanier area: the axial planes are variable in orientation, but commonly dip shallowly towards the north to northwest, with fold axes nearly coaxial with F_3.

FOLD GEOMETRY

Figure 4 is a detailed sketch of the analysed fold. The folded schistosity is the regionally dominant planar foliation S_2, and is defined by sub-parallel white mica, biotite, platy quartz, zoisite, tourmaline and opaque minerals. Lithological layering, where discernible around the fold, is effectively parallel to S_2. Overall, the fold has a chevron fold-style with relatively long straight limbs and a rather narrow sharp hinge. The P_1 value, as defined by Ramsay (1967, p. 350), lies between 4.5 and 5. According to the classification of Fleuty (1964), the fold is 'close', having an interlimb angle of between 55°

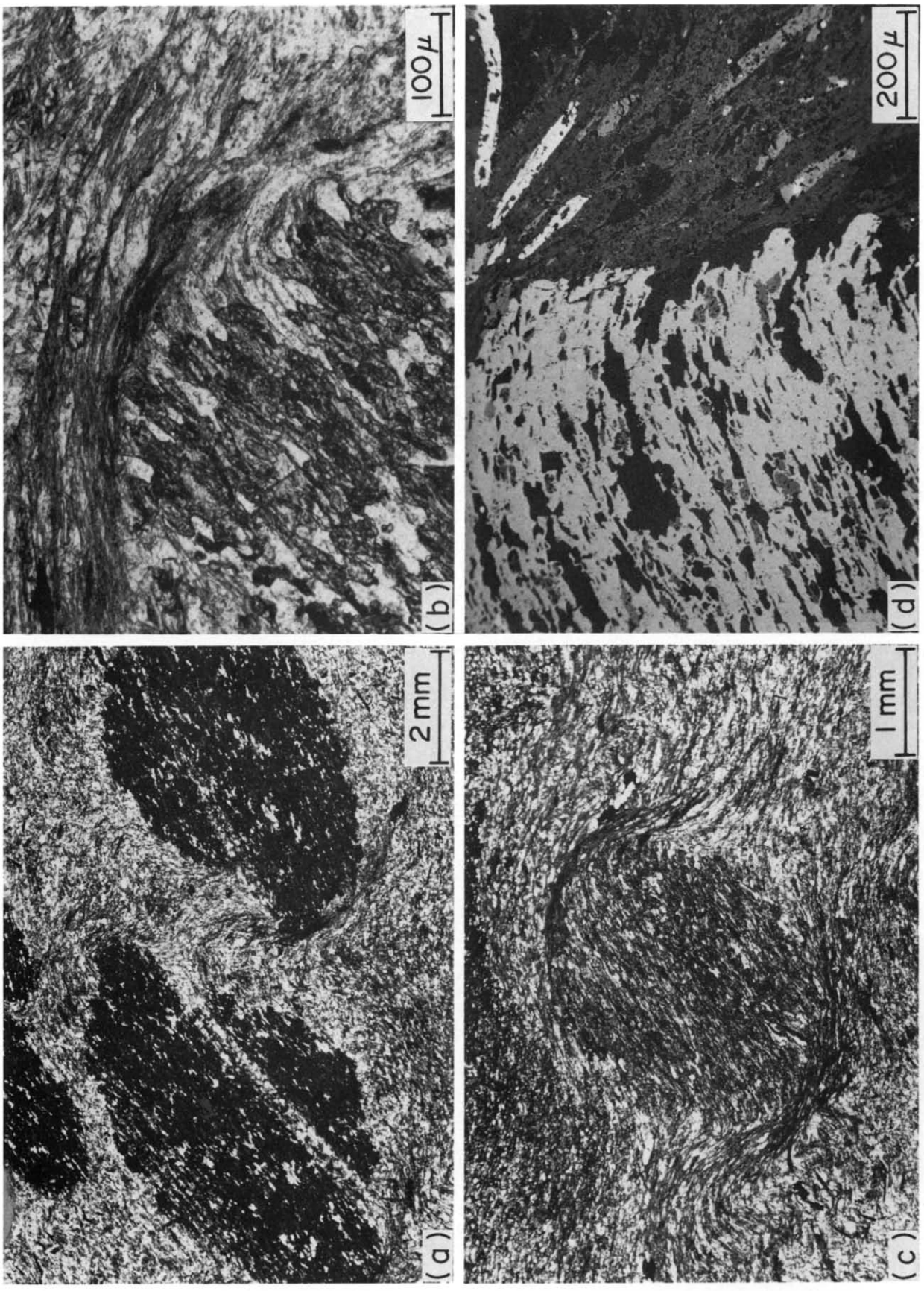

Fig. 2. Internal–external foliation relationships for the garnet porphyroblasts. (a) Photomicrograph, with crossed nicols, of typical garnet porphyroblasts with a straight internal foliation. Note the difference in orientation of S_i between adjacent porphyroblasts. (b) Photomicrograph of the rim of one of the same porphyroblasts, with plane light, showing the continuity of the external and internal foliation, but with an abrupt change in orientation going from S_i to S_e. (c) Photomicrograph, with plane light, of a garnet porphyroblast showing the less common development of a narrow rim where S_i bends rapidly but continuously into S_e. (d) Backscatter image from the electron microprobe of the same porphyroblast, showing the continuity of the external and internal foliation and the rapid bending of the foliation in a narrow rim. The light-coloured elongate minerals in the matrix are zoisite.

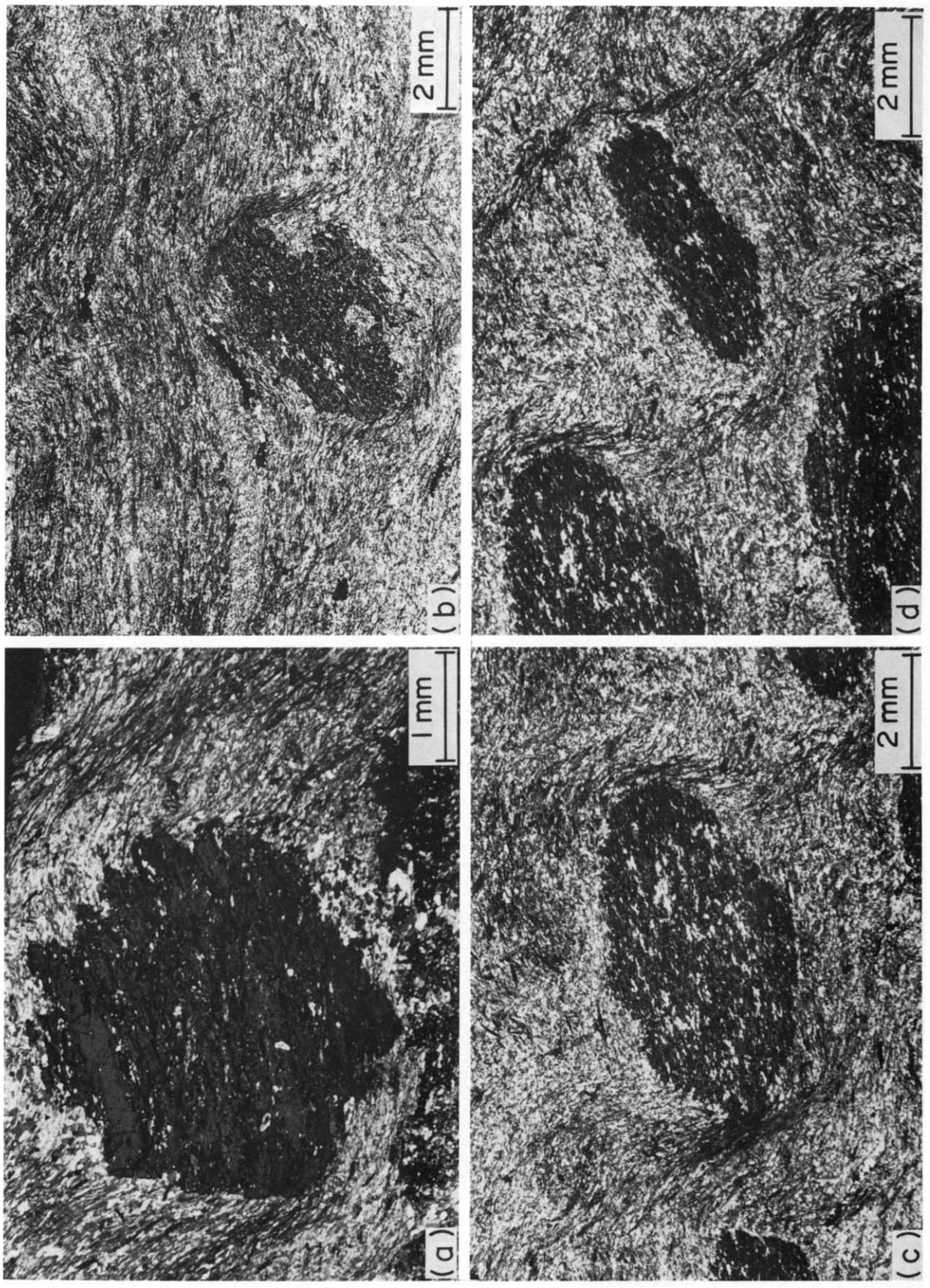

Fig. 3. Photomicrographs showing the variation in ellipticity (aspect ratio) of garnet porphyroblasts and the relationship between S_i and S_e. The aspect ratio of the porphyroblast in (a) is 1.06. in (b) is 1.6, in (c) is 1.9 and in (d) is 2.5.

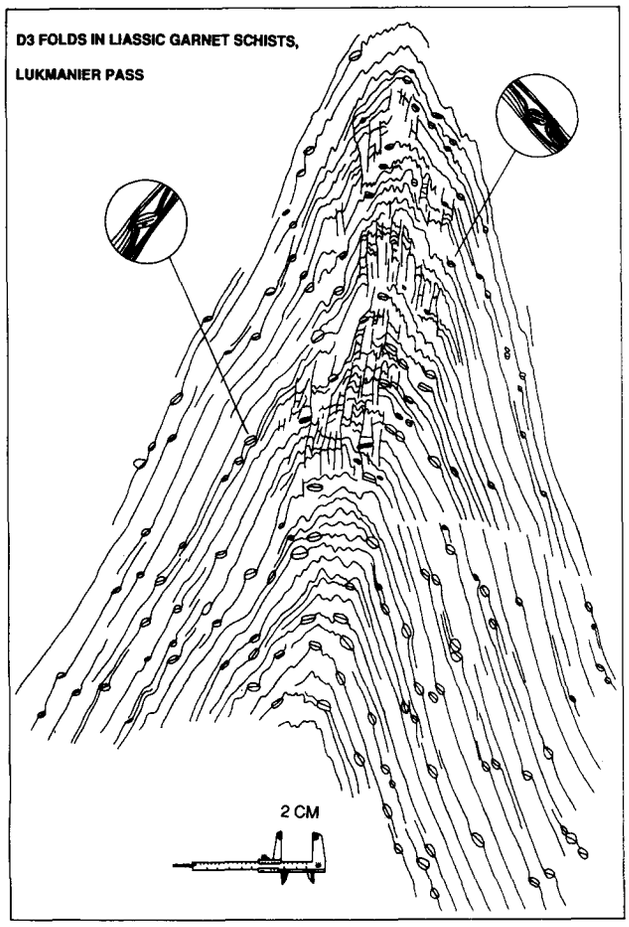

Fig. 4. Sketch of the folded schistosity and porphyroblast distribution around the fold. Enlargements within the circles show the typical geometry observed on each limb of the fold.

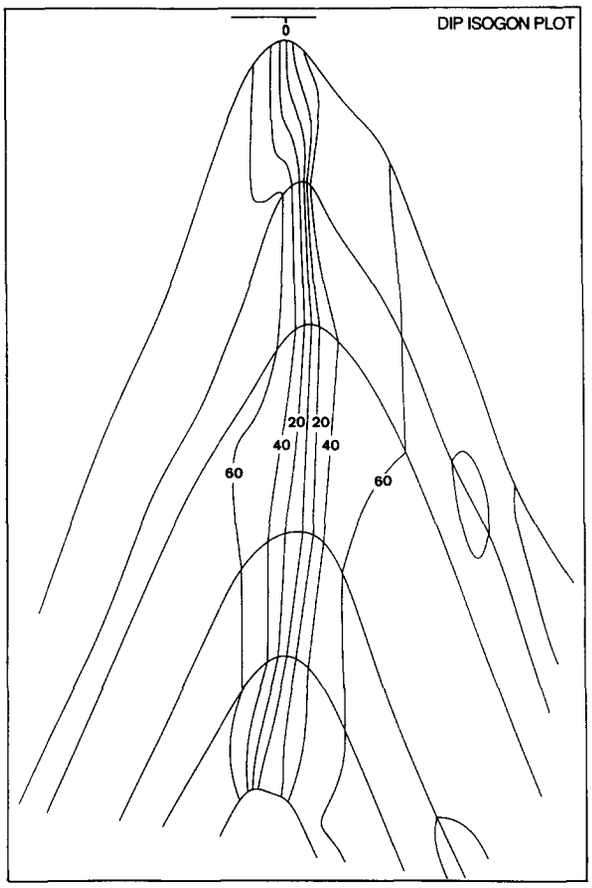

Fig. 5. Dip isogon construction for the fold. Smoothing was achieved using a tight cubic-spline function and dip isogons were constructed using a simple contouring routine on a microcomputer. The dip at the hinge (point of maximum curvature) is arbitrarily taken as zero.

and 60°. From the dip isogons (Fig. 5), it can be seen that the fold geometry approximates that of a similar or Type 2 fold of Ramsay (1967, p. 365), with local variation along the axial surface between Type 1C and Type 3.

PORPHYROBLAST GEOMETRY

Data collection

The ellipticity of each garnet (determined with the aid of callipers) together with the dip of S_i and S_e (dip at the fold hinge taken as zero) were measured on a near planar joint surface, which makes an angle of 75° with the fold axis. The apparent dips measured on this joint surface will never differ from the true dips in the fold profile plane by more than 1° (cf. fig. 1.8 of Ragan 1968), and this small difference can be reasonably ignored. The garnet porphyroblasts usually have lengths between 5 and 10 mm, and widths between 2 and 6 mm (Figs. 2 and 3). A few smaller porphyroblasts could not be accurately measured and are not included in the data. Measurements on garnet couplets, which have coalesced during growth, give anomalously low values of relative rotation, as do measurements on garnet porphyroblasts with very near neighbours (on the order of the porphyroblast dimensions). The anomalous results reflect the effects of interaction (e.g. Ildefonse *et al.* 1992). These few results have also been excluded from the analysis.

Results

The measurements of porphyroblasts around the fold are presented in Fig. 6 as a plot of the dip of S_i against the dip of S_e, for different ranges of porphyroblast ellipticity (given as the axial ratio). The dip of the straight internal foliation S_i can usually be measured quite accurately (to within 2–3°), whereas the variation in orientation of S_e due to open crenulations results in lower precision and the average orientation around each porphyroblast can generally only be determined to within about 5°. Repeat measurements of the axial ratio of the porphyroblasts are accurate to the first decimal place. The raw data have been smoothed by considering a moving window of external dip values, 10° wide, and plotting the average value of the internal dip within this range, together with error bars representing the standard deviation of the averaged values (Fig. 6). These plots show that the dip of S_i is generally less than the dip of S_e (i.e. there has been a relative rotation) and that the dip of S_i increases consistently with the dip of S_e, particularly for the more elongate garnet porphyroblasts (e.g. Fig. 6e). The dip of S_i thus depends both on the position of the porphyro-

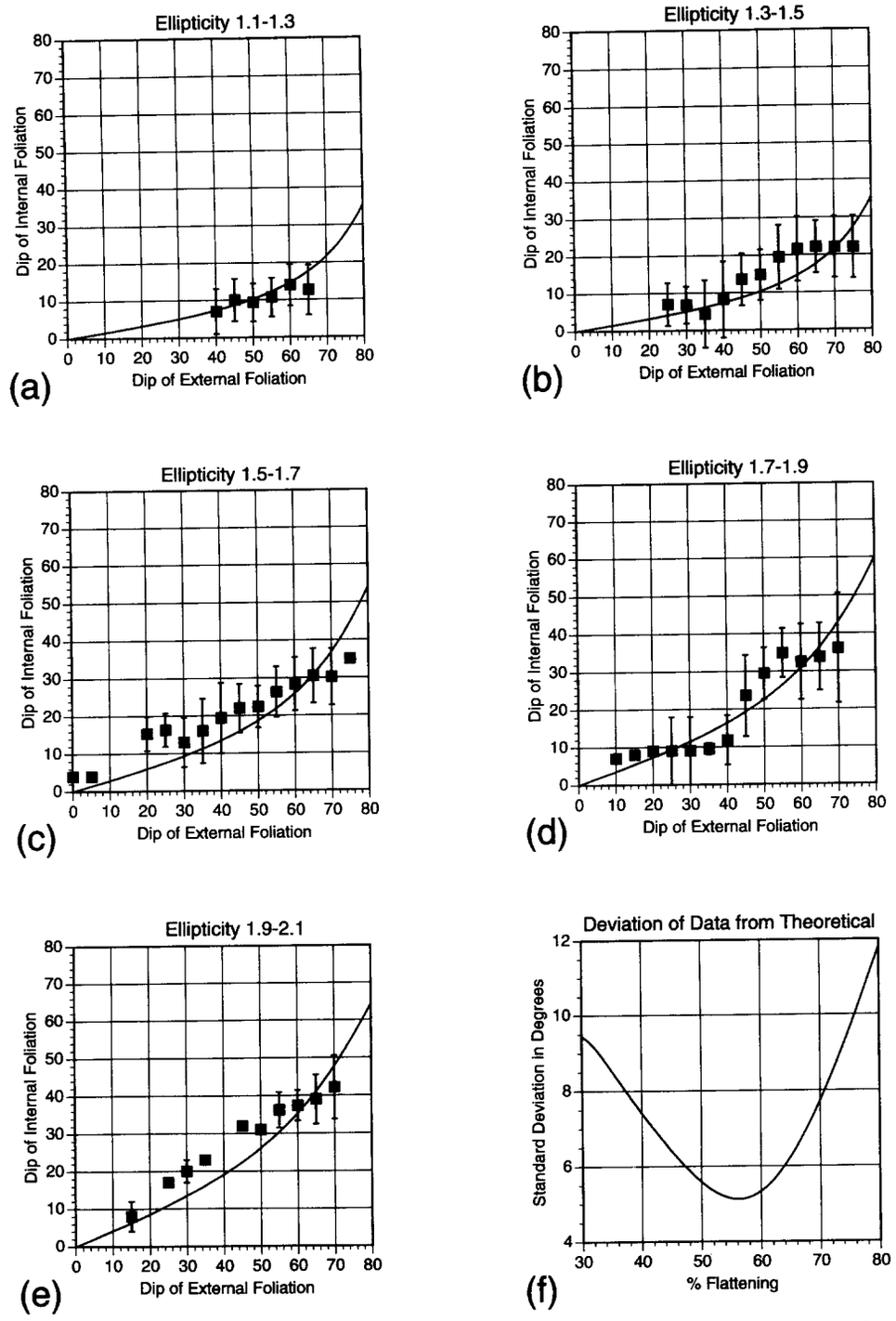

Fig. 6. (a)–(e) Plots of dip of the helicitic internal foliation in the garnet porphyroblasts vs dip of the immediately adjacent external foliation. The data have been smoothed by taking average values of the dip of the internal foliation for a moving 10° window of values of the dip of the external foliation. Bars correspond to the standard deviation for these averaged values. Bars are absent when only one value was available. Ellipticity 1.1–1.3, 18 data; 1.3–1.5, 85 data; 1.5–1.7, 102 data; 1.7–1.9, 49 data; 1.9–2.1, 26 data. Solid curves correspond to the best-fit theoretical results for a flexural flow fold flattened 56% (see f and text). (f) Residual standard deviation between theoretical and measured values, i.e.

$$\sqrt{\Sigma\,(\text{data value} - \text{theoretical value})^2/(\text{total number of data} - 1)}$$

as a function of % homogeneous shortening in a flattened flexural flow model (see text). The minimum corresponds to the curves plotted in (a)–(e).

blast within the fold (as given by the dip of the external foliation S_e) and on the ellipticity of the porphyroblast.

The average dip of the internal foliation, for a particular range of porphyroblast ellipticities, can also be directly represented as trajectories across the fold (Fig. 7). The internal foliation describes a fold, but with a greater opening angle than the fold in the external schistosity. The opening angle of this fold in the internal foliation decreases as the ellipticity of the porphyroblasts increases. Indeed, the external schistosity is itself defined by the preferred orientation of white mica, biotite and zoisite, which also grew prior to folding (they are bent around the crenulations) and themselves represent stiff inclusions within the more quartzo-

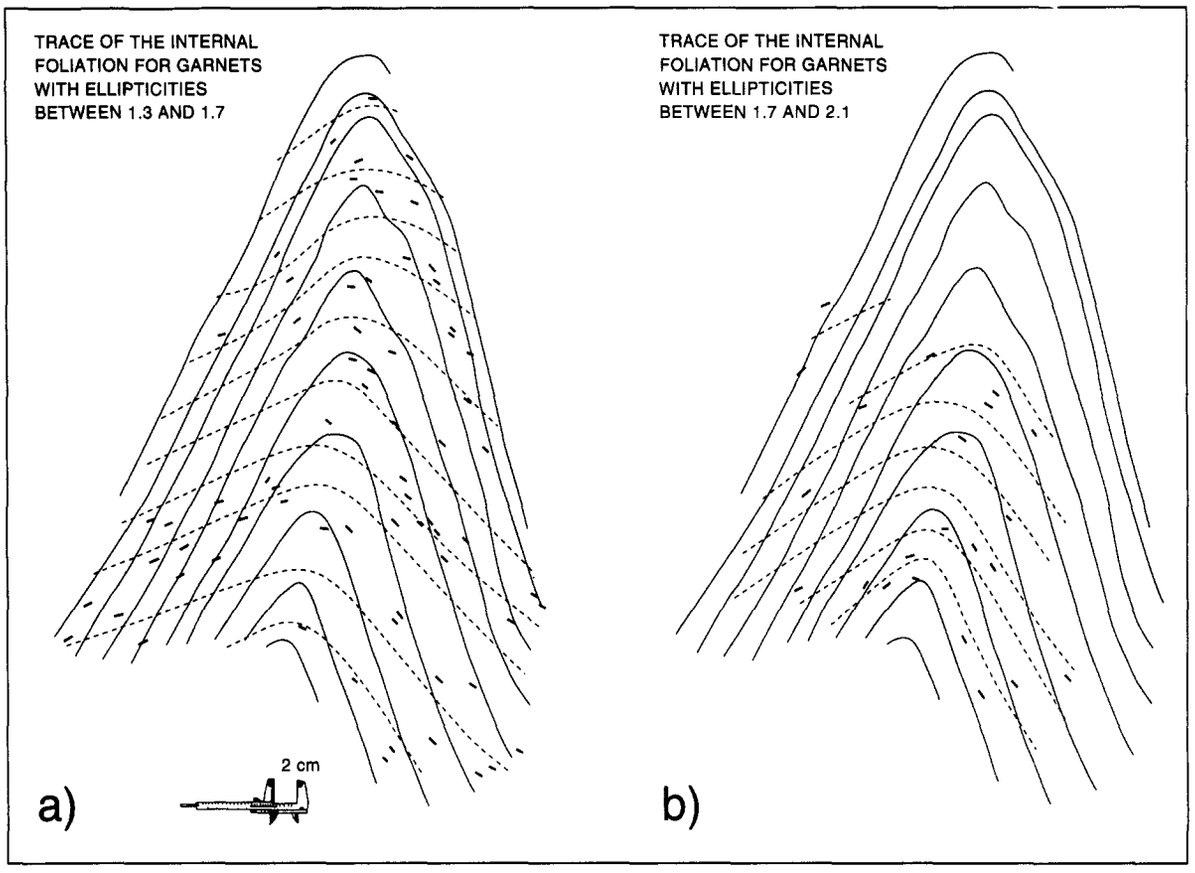

Fig. 7. Trace of the average orientation of S_i within the garnet porphyroblasts (dashed lines) vs the shape of the fold in the external schistosity S_e (solid lines). (a) For porphyroblasts with ellipticities in the range 1.3–1.7. (b) For porphyroblasts with ellipticities in the range 1.7–2.1.

feldspathic matrix during folding. These matrix minerals have a high aspect ratio (>*ca* 7:1, cf. Fig. 2), markedly higher than the garnet porphyroblasts, and the opening angle of the fold in the external foliation, defined by these elongate minerals, is correspondingly smaller. Interference effects between such platy grains in a concentrated population will also have a marked effect on their rotational behaviour, in general tending to slow down their rotation (Ildefonse & Fernandez 1988).

PORPHYROBLAST CHEMISTRY

The chemistry of four garnet porphyroblasts in the same sample taken from the limb of the measured fold has been determined with an electron microprobe in a series of traverses parallel to the internal foliation. The major element chemistry is very homogeneous and all the measured garnet porphyroblasts have calculated compositions (±1 SD) in the range 70.0 ± 1.1% almandine, 16.8 ± 1.9% grossular, 7.3 ± 0.7% pyrope, 2.3 ± 0.4% spessartine and 3.1 ± 1.9% andradite. The only consistent variation appears to be in the spessartine component, although this is a small variation in an already small quantity and caution is required. The variation in spessartine content with orientation of S_i is plotted in Fig. 8(a). Only one of the measured garnets (that plotted with a square symbol in Fig. 8) has a well developed rim in which S_i is dramatically bent through about 70° (cf. Fig. 2d). For this garnet, there is a good correlation between the orientation of S_i and the measured spessartine content (Fig. 8a), with a rim composition of ~3.2% spessartine and a core of 1.8–2.0%. The other three garnets have only weakly developed rims and the spessartine content varies only within a narrow range of ~1.8–2.3%, despite a variation in geographic orientation of the straight internal foliation S_i of more than 40°. This constancy of the core composition irrespective of S_i orientation is emphasized in Fig. 8(b), where the spessartine content is plotted against the difference in angle between local S_i and the S_i orientation within the straight core region. The chemical analyses do not, therefore, suggest that there was sequential growth of porphyroblasts over a progressively rotated foliation, but rather that the garnet cores grew more or less contemporaneously, and that the currently observed variation in orientation of S_i within these cores is due to their subsequent rotation as rigid inclusions.

FOLD MODEL

The fold was initiated in an already strongly schistose rock and developed a chevron-style fold geometry with a narrow hinge zone and long, rather straight limbs. This geometry is typical of folds developed in strongly anisotropic rocks in which the fold mechanism approaches that of flexural flow, with the limb rotation accommo-

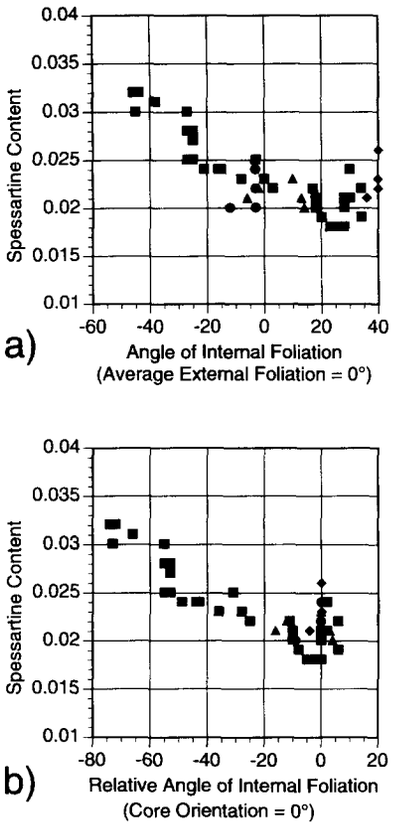

Fig. 8. Variation in spessartine content with orientation of S_i in four garnet porphyroblasts. (a) Spessartine content (mole fraction) vs orientation of S_i relative to a fixed reference system (parallel to the average orientation of the external foliation S_e, i.e. average orientation of S_e is taken as 0°). The S_i orientation in the volumetrically dominant core region is 28° for the garnet with the square symbol, −3° for the circle, 10° for the triangle, and 40° for the diamond. Positive angles correspond to the sense of relative rotation as shown in the circled enlargements of Fig. 4. (b) Spessartine content (mole fraction) vs angular difference between local S_i and S_i in the core of the porphyroblast.

dated by simple shear (e.g. Cobbold 1976, Ramsay & Huber 1987, fig. 20.11). As derived by Ramsay & Huber (1987, equation 21.5), the amount of simple shear (γ) is equal to the limb dip in radians (taking the dip at the hinge to be zero). The expected amount of finite rotation for rigid porphyroblasts with differing axial ratios (taken as initially elongate parallel to the external foliation) can then be readily calculated for values of simple shear corresponding to the respective limb dips (e.g. Ghosh & Ramberg 1976, Fernandez 1988). The results are presented in Fig. 9(a), as plots of internal vs external foliation, similar to Fig. 6.

Flexural flow folding results in parallel, Type 1B folds. However, as the limbs rotate the amount of shortening accommodated by such a folding mechanism decreases and further shortening may be accommodated by a more homogeneous flattening of the whole fold. Such homogeneous flattening modifies the fold geometry towards a similar, Type 2 fold style (Ramsay 1962), and the amount of flattening required can be estimated from plots of layer thickness variation with limb dip (e.g. Ramsay 1967, fig. 7–79). In practice, the estimation becomes increasingly inaccurate as the fold geometry more closely approaches that of similar geometry, as is the case here. Although some 'layers' in Fig. 5, defined by smoothed trajectories to the folded schistosity, have a Type 1C geometry, they cannot really be related to specific competent compositional layers and a quantitative determination of the amount of flattening cannot be justified. Only a qualitative comparison of the observed porphyroblast behaviour with the predicted behaviour around a flattened flexural fold can be made.

A simple two-stage model for the development of a flattened flexural flow fold has been used. The homogeneous flattening component is first removed by pure shear 'unstraining' to obtain the fold geometry after flexural flow but prior to flattening. The rotation of porphyroblasts due to the flexural flow component is then calculated as a function of the limb dip prior to flattening (cf. Fig. 9a). The additional rotation due to the pure shear flattening component is then calculated, to give the final porphyroblast orientation about the flattened flexural flow fold. A value of 50% for the flattening component is chosen for Fig. 9(b), as this produces calculated curves which are a good approximation to the data presented in Fig. 6. The 'best-fit' to the data of Fig. 6 actually occurs when the flattening component is ~56% (Fig. 6f), but the minimum is not so tightly constrained that the flattening component can be determined to such accuracy.

As shown in Fig. 9, porphyroblasts with high aspect ratio (>5) behave very much like passive marker lines (e.g. Ghosh & Ramberg 1976) and show very little rotation relative to the external foliation. This remains true whether a homogeneous flattening component is added or not (compare Fig. 9a with 9b). However, for less elongate porphyroblasts, the dip of S_i should always be less than the dip of S_e, and this effect becomes more marked as the ellipticity decreases and the component of homogeneous flattening increases (Figs. 9 and 10). These theoretical results are in good qualitative agreement with the measurements from the natural example, as can be seen from a comparison between the measured data and the theoretical curves presented in Fig. 6.

The variation in dip of S_i for nearly circular porphyroblasts in strongly flattened folds approaching similar geometry may be small, even when the folds themselves are tight (e.g. variation of only ± 12° where limb dips reach 60°, as shown in Figs. 9b and 10). As the ellipticity of the porphyroblasts increases, however, the variation in the orientation of S_i should become more significant (e.g. Fig. 10), as is observed in the measured natural example. For porphyroblasts with axial ratios greater than around 5:1, there should be no appreciable rotation relative to the external foliation. In the natural example, isolated zoisite porphyroblasts (ellipticities >10:1) indeed help define the folded main foliation and do not show discernible relative rotation (e.g. Fig. 2d).

CONCLUSIONS

Measurements of orientation of the internal foliation within garnet porphyroblasts demonstrate a very clear

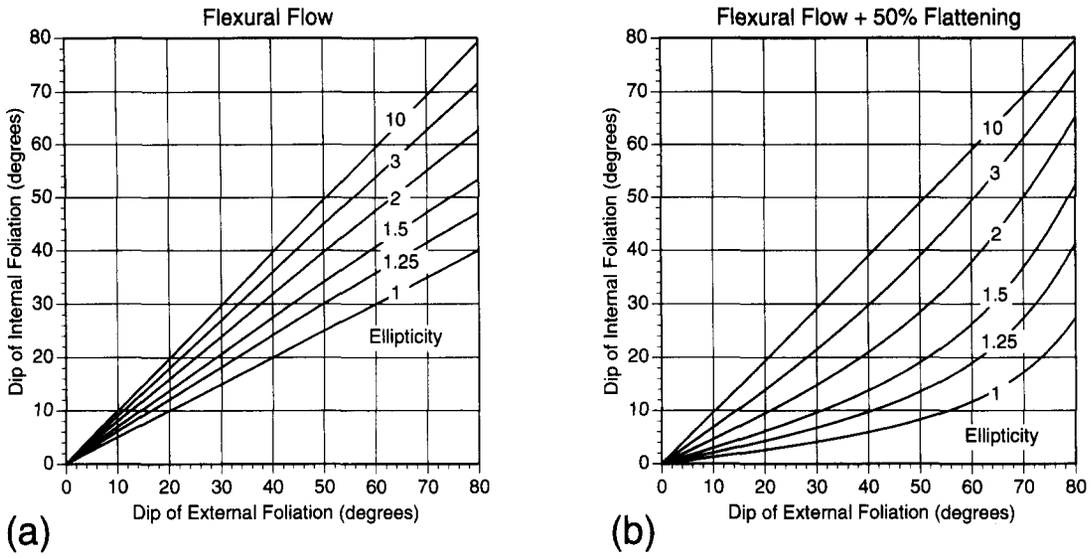

Fig. 9. (a) Theoretical curves for the dip of S_i vs S_e for a flexural flow fold model. (b) Theoretical curves for the dip of S_i vs S_e for a two-stage flattened flexural flow fold model, in which initial flexural flow folding is followed by a 50% homogeneous flattening.

dependence on position within the fold (as given by the dip of the external foliation) and on the ellipticity. This consistent variation cannot be explained by any model which assumes *a priori* the non-rotation of porphyroblasts relative to geographic co-ordinates (e.g. Bell 1985, Bell & Johnson 1989, 1990, Johnson 1990); it can readily be explained in terms of the classical theories of rigid-body rotation (e.g. Jeffery 1922, Ghosh & Ramberg 1976, Fernandez 1988). Regardless of the chosen folding model, finite strain varies in a systematic manner with position around the fold, and the variation in finite rotation of rigid particles is a function of both the finite strain and the particle ellipticity. As discussed above, flattened flexural flow folding can qualitatively explain the observed variation in orientation of the porphyroblast internal foliation. In particular, relatively equant inclusions in strongly flattened folds may show only limited variation in the orientation of the internal foliation even when folding is quite tight (Figs. 7, 9 and 10). However, even this slight variation may still be discernible and should be consistent with the position of the porphyroblast within the fold (Figs. 7 and 10). The observations of Fyson (1980, fig. 2) on the limited regional variation in orientation of the internal foliation preserved within rather equant biotite porphyroblasts (Fyson 1980, figs. 4 and 5) are reproduced in slightly simplified form in Fig. 11. These results have been cited as evidence for the non-rotation of porphyroblasts (e.g. Bell & Johnson 1990), but as can be seen from Fig. 11, there is in fact a rather consistent variation in the orientation of the internal foliation identical in form to that of Figs. 7 and 10. As demonstrated here, this cannot be used as evidence for general non-rotation of porphyroblasts, but only reflects the specific conditions of nearly equant rigid inclusions involved in deformation with a weak rotational component (e.g. Ramsay 1962, Ghosh & Ramberg 1976, Passchier 1987). As proposed

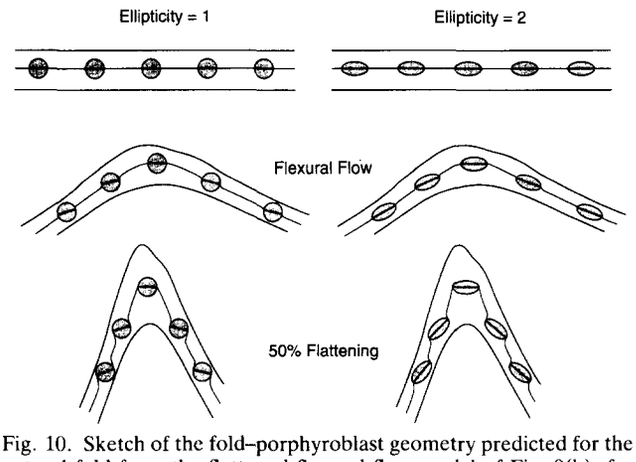

Fig. 10. Sketch of the fold–porphyroblast geometry predicted for the natural fold from the flattened flexural flow model of Fig. 9(b), for initial circular objects (ellipticity = 1) and elliptical objects initially elongate parallel to the foliation with axial ratio of 2:1. The final fold geometry can be directly compared to that of Fig. 4.

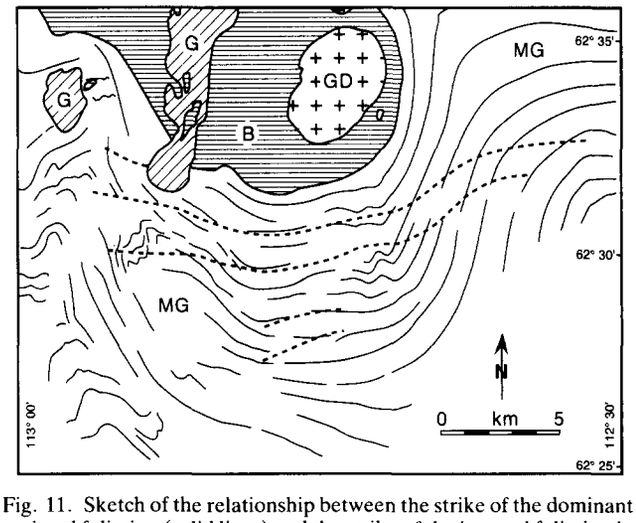

Fig. 11. Sketch of the relationship between the strike of the dominant regional foliation (solid lines) and the strike of the internal foliation in biotite porphyroblasts (short dotted lines) in Archean rocks near Yellowknife, Northwest Territories, Canada. Simplified after fig. 2 from Fyson (1980). (G: granite; GD: granodiorite; MG: metagreywacke, argillite, schist; B: basalt, andesite, dacite, rhyolite.) Published with permission of the National Research Council of Canada.

theoretically (Jeffery 1922, Gay 1968, Ghosh & Ramberg 1976, Ferguson 1979, Fernandez 1988), demonstrated experimentally (Ghosh & Sengupta 1973, Ghosh & Ramberg 1976, Fernandez *et al.* 1983, Van Den Driessche & Brun 1987, Ildefonse & Fernandez 1988, Ildefonse *et al.* 1992) and confirmed in the natural fold example of this study, the behaviour of individual rigid inclusions depends both on the shape of the particle itself and on the deformational history, reflected in this particular natural example by differences in strain history with position about the fold.

Acknowledgements—Discussions with Tim Bell, Martin Casey, Benoît Ildefonse, Cees Passchier, and John Ramsay were greatly appreciated in developing the ideas presented here. Constructive and thorough reviews by Angel Fernandez and Ron Vernon also helped improve the presentation. Eric Reusser is thanked for his help with electron microprobe analyses. Peter Visser was supported financially in his doctorate work by the Swiss Nationalfonds (Project No. 20-27462.89).

REFERENCES

Adams, H. G., Cohen, L. H. & Rosenfeld, J. G. 1975. Solid inclusion piezothermometry: II. Geometric basis, calibration for the association quartz–garnet, and application to some pelitic schists. *Am. Miner.* **60**, 584–598.

Bell, T. H. 1985. Deformation partitioning and porphyroblast rotation in metamorphic rocks: a radical reinterpretation. *J. metamorph. Geol.* **3**, 109–118.

Bell, T. H. & Johnson, S. E. 1989. Porphyroblast inclusion trails: the key to orogenesis. *J. metamorph. Geol.* **7**, 279–310.

Bell, T. H. & Johnson, S. E. 1990. Rotation of relatively large rigid objects during ductile deformation: well established fact or intuitive prejudice? *Aust. J. Earth Sci.* **37**, 441–446.

Bell, T. H. & Johnson, S. E. 1992. Shear sense: a new approach that resolves problems between criteria in metamorphic rocks. *J. metamorph. Geol.* **10**, 99–124.

Chadwick, B. 1965. The structural and metamorphic geology of the Lukmanier region. Unpublished Ph.D. thesis, University of London.

Cobbold, P. R. 1976. Mechanical effects of anisotropy during large finite deformations. *Bull. Soc. géol. Fr.* **18**, 1497–1510.

Ferguson, C. C. 1979. Rotations of elongate rigid particles in slow non-newtonian flows. *Tectonophysics* **60**, 247–262.

Fernandez, A. 1988. Strain analysis from shape preferred orientation in magmatic rocks. *Bull. geol. Inst. Univ. Uppsala* **14**, 61–67.

Fernandez, A., Feybesse, J. L. & Mezure, J. F. 1983. Theoretical and experimental study of fabric developed by different shaped markers in two-dimensional simple shear. *Bull. Soc. géol. Fr.* **25**, 319–326.

Fleuty, M. J. 1964. The description of folds. *Proc. Geol. Ass.* **75**, 461–489.

Fox, J. S. 1974. Petrology of some low-variance meta-pelites from the Lukmanier Pass area, Switzerland. Unpublished Ph.D. thesis, Cambridge University.

Fox, J. S. 1975. Three-dimensional isograds from the Lukmanier Pass, Switzerland, and their tectonic significance. *Geol. Mag.* **112**, 547–564.

Frey, M. 1978. Progressive low grade metamorphism of a blackshale formation, Central Swiss Alps, with special reference to pyrophyllite and margarite bearing assemblages. *J. Petrol.* **19**, 95–135.

Frey, M., Bucher, K., Frank, E. & Mullis, J. 1980. Alpine metamorphism along the Geotraverse Basel-Chiasso: a review. *Eclog. geol. Helv.* **73**, 527–546.

Fyson, W. K. 1975. Fabrics and deformation of Archean metasedimentary rocks, Ross Lake–Gordon Lake area, Slave Province, Northwest Territories. *Can. J. Earth Sci.* **12**, 765–776.

Fyson, W. K. 1980. Fold fabrics and emplacement of an Archean granitoid pluton, Cleft Lake, Northwest Territories. *Can. J. Earth Sci.* **17**, 325–332.

Gay, N. C. 1968. Pure shear and simple shear deformation of inhomogeneous viscous fluids. I—Theory. *Tectonophysics* **5**, 211–234.

Ghosh, S. K. & Ramberg, H. 1976. Reorientation of inclusions by combination of pure shear and simple shear. *Tectonophysics* **34**, 1–70.

Ghosh, S. K. & Sengupta, S. 1973. Compression and simple shear of test models with rigid and deformable inclusions. *Tectonophysics* **17**, 133–175.

Ildefonse, B. & Fernandez, A. 1988. Influence of concentration of rigid markers in a viscous medium on the production of preferred orientations. An experimental contribution. 1. Non coaxial strain. *Bull. geol. Inst. Univ. Uppsala* **14**, 55–60.

Ildefonse, B., Sokoutis, D. & Mancktelow, N. S. 1992. Mechanical interactions between rigid particles in a deforming ductile matrix. Analogue experiments in simple shear flow. *J. Struct. Geol.* **14**, 1253–1266.

Jeffery, G. B. 1922. The motion of ellipsoidal particles immersed in a viscous fluid. *Proc. R. Soc. Lond.* **A102**, 161–179.

Johnson, S. E. 1990. Lack of porphyroblast rotation in the Otago schists, New Zealand: implications for crenulation cleavage development, folding and deformation partitioning. *J. metamorph. Geol.* **8**, 13–30.

Mügge, O. 1930. Bewegungen von Porphyroblasten in Phylliten und ihre Messung. *Neues Jb. Miner. Geol. Paläont. Mh.* **61A**, 469–510.

Olesen, N. O. 1978. Distinguishing between interkinematic and synkinematic porphyroblastesis. *Geol. Rdsch.* **67**, 278–287.

Passchier, C. W. 1987. Stable positions of rigid objects in non-coaxial flow—a study in vorticity analysis. *J. Struct. Geol.* **9**, 679–690.

Passchier, C. W. & Simpson, C. 1986. Porphyroclast systems as kinematic indicators. *J. Struct. Geol.* **8**, 831–843.

Ragan, D. M. 1968. *Structural Geology*. John Wiley, New York.

Ramsay, J. G. 1962. The geometry and mechanics of formation of 'similar' type folds. *J. Geol.* **70**, 309–327.

Ramsay, J. G. 1967. *Folding and Fracturing of Rocks*. McGraw-Hill, New York.

Ramsay, J. G. & Huber, M. I. 1987. *The Techniques of Modern Structural Geology, Volume 2: Folds and Fractures*. Academic Press, London.

Rosenfeld, J. L. 1968. Garnet rotations due to the major Paleozoic deformations in southeast Vermont. In: *Studies of Appalachian Geology: Northern and Maritime* (edited by Zen, E., White, W. S., Hadley, J. B. & Thompson, J. B., Jr). John Wiley, New York, 185–202.

Rosenfeld, J. L. 1970. Rotated garnets in metamorphic rocks. *Spec. Pap. geol. Soc. Am.* **129**.

Schmidt, W. 1918. Bewegungsspuren in Porphyroblasten Kristalliner Schiefer. *Sb. Akad. Wiss. Wien, Abt.* **127**, 293–310.

Schoneveld, C. 1977. A study of some typical inclusion patterns in strongly paracrystalline rotated garnets. *Tectonophysics* **39**, 453–471.

Schoneveld, C. 1979. The geometry and the significance of inclusion patterns in syntectonic porphyroblasts. Unpublished Ph.D. thesis, University of Leiden.

Simpson, C. & Schmid, S. M. 1983. An evaluation of criteria to deduce the sense of movement in sheared rocks. *Bull. geol. Soc. Am.* **94**, 1281–1288.

Spry, A. 1963. The origin and significance of snowball structure in garnet. *J. geol. Soc. Aust.* **10**, 193–208.

Spry, A. H. 1969. *Metamorphic Textures*. Pergamon Press, Oxford.

Steinhardt, C. K. 1989. Lack of porphyroblast rotation in non-coaxially deformed schists from Petrel Cove, South Australia, and its implications. *Tectonophysics* **158**, 127–140.

Thakur, V. C. 1973. Events in Alpine deformation and metamorphism in the N. Alpine zone and S. Gotthard Massif regions. *Geol. Rdsch.* **62**, 549–563.

Truesdell, C. 1954. *The Kinematics of Vorticity*. Indiana University Press, Bloomington.

Van Den Driessche, J. & Brun, J.-P. 1987. Rolling structures at large shear strain. *J. Struct. Geol.* **9**, 691–704.

Vernon, R. H. 1987. A microstructural indicator of shear sense in volcanic rocks and its relationship to porphyroblast rotation in metamorphic rocks. *J. Geol.* **95**, 127–133.

Vernon, R. H. 1988. Microstructural evidence of rotation and non-rotation of mica porphyroblasts. *J. metamorph. Geol.* **6**, 595–602.

Zwart, H. J., 1960. Relations between folding and metamorphism in the Central Pyrenees and their chronological succession. *Geologie Mijnb.* **39**, 163–180.

Zwart, H. J. & Oele, J. A. 1966. Rotated magnetite crystals from the Rocroi Massif (Ardennes). *Geologie Mijnb.* **45**, 70–74.